CHAPTER 5

To encapsulate phytochemical extract of edible flower and their characterization

5.1. Introduction

Phlogacanthus thyrsiflorus also known as Nongmangkha which is an edible flower a traditional delicacy of various parts of India. It belongs to the acanthaceae family. It is believed to confer medicinal effects such as prevent skin diseases (sore, scabies etc.), cure pox, wounds, tumors, kidney stone, liver disorder and also work as blood purifier etc. (Koushik et al., 2020, Das et al., 2017). Various studies reported the presence of steroids, terpenoids, flavonoids and phenol, antioxidant and radical scavenging activities hypoglycemic and hypolipidemic properties (Nongthombam et al., 2018a, 2018b, Ahmed et al., 2016). Hence, it is beneficial to consume the flowers of Nongmangkha. Edible flowers have very low shelf life which limits the commercial viability of edible flowers and to overcome this limitation one of the ways we can follow is to extract the nutritional part from edible flowers and can utilize for further use such as formulation of functional food products etc. But the direct use of the flower extract might cause degradation of bioactive compounds of the extract as some of these compounds are not stable in some environmental conditions. This might be due to various factors such as light, pH, temperature and storage condition etc. along with simulated gastrointestinal digestion affects to decrease the levels of polyphenols or bioavailability of it or the quality of a polyphenol rich or bioactive compounds rich extract can be graded and resulting it loss of quality of an extract (Pasukamonset et al., 2016). Therefore, adapting encapsulation is one of the techniques which can cut these losses, preserve and provide stability of bioactive compounds.

Phlogacanthus thyrsiflorus, also known as Nongmangkha, is an edible flower used as a traditional culinary delicacy in various parts of India. It belongs to the acanthaceae family and is believed to confer a basket of medicinal benefits, such as prevention of skin diseases (sore, scabies etc.); treatment and cure for pox, wounds, tumors, kidney stone, liver disorder; and also work as a blood purifier, etc. (Koushik et al., 2020; Das et al., 2017). Various studies revealed the presence of steroids, terpenoids, flavonoids and phenol, antioxidant activities, accompanied by hypoglycemic and hypolipidemic effects etc. (Nongthombam et al., 2018a, 2018b; Ahmed et al., 2016). The benefits of consumption of Nongmangkha flowers are well described in existing

literature. However, edible flowers are highly perishable, which restricts their commercial viability. Preparation of an extract of nutritional parts of edible flower for further use and preservation is one of the ways to circumvent the issue. Despite its therapeutic potential, the direct use of Nongmangkha flower extract in functional foods or supplements is limited by the instability of its bioactive compounds under environmental and gastrointestinal conditions. Phenolic compounds are highly susceptible to degradation due to light, heat, pH changes, and enzymatic activity during digestion, resulting in reduced bioavailability and diminished biological efficacy (Pasukamonset, et al., 2016). Also, direct use of flower extract might alter the taste of food and other sensory attributes. To address this challenge, the present study investigates the encapsulation of perishable Nongmangkha flower extract using an alginate-based ionic gelation technique. Encapsulation serves as a protective strategy to enhance stability, control release, and improve gastrointestinal retention of phenolic compounds, thereby increasing their functional potential in nutraceutical and food applications.

Encapsulation has been documented to provide a prolonged and controlled release of polyphenols or other active compounds and hence regarded as a good delivery system of bioactive compounds (Stojanovic et al., 2012). Some examples of encapsulation techniques are spray drying, solvent evaporation, coacervation, freeze drying and ionic gelation, interfacial polymerization etc. (Santana et al., 2023). Ionic gelation is a technique used to create hydrogels or nanoparticles by the electrostatic interaction between oppositely charged molecules. This process involves the crosslinking of a polymer with counter ions, such as polyvalent ions, which leads to the formation of a gel (Patil et al, 2012). So, ionic gelation is one of the encapsulation techniques which can be adopted to protect the quality as well as bioavailability of active compounds and is considered as a simple and low-cost technique (Kurozawa et al., 2017). Alginate is a non-toxic hydrophilic polymer, also biodegradable and biocompatible with a capacity to form spontaneous gelation when in contact with divalent cations such as Ca^{2+}ions (Grant et al., 1973 and George et al., 2006). Alginate can be obtained from bacteria, marine brown algae, and other sources etc. Sodium alginate, the sodium salt derived from alginic acid, consists of β-D-mannuronic and α-D-guluronic units connected by 1,4-glycosidic linkages. Based on the source of polysaccharide, the composition and patterning of the monomers varies.

In this study, sodium alginate (a biodegradable polysaccharide) was used for encapsulation, resulting in a gel structure that resembles an 'egg-box' (Patel et al. 2016). Polyphenol-rich extract of Nongmangkha flower was obtained by using microwave assisted extraction technique (MAE). The combination of microwave-assisted extraction (MAE) and ionic gelation encapsulation offers a novel and synergistic approach for maximizing recovery and stability of heat-sensitive bioactive compounds from plant materials. MAE is known for its ability to enhance extractability by disrupting plant cell walls through rapid internal heating, thereby improving the release of phenolics and other phytochemicals. However, it is possible that the thermal exposure during MAE may pose risks to certain bioactive compounds. Therefore, integrating ultrasound pretreatment prior to MAE has been reported to further improve extraction yields by non-thermally weakening cell wall structures, as demonstrated in studies involving pectin, isoflavones, and phenolics (Bagherian et al., 2011; Pananun et al., 2012; Izadifar 2013 and Pongmalai et al., 2013). So, the main objective of this study was to optimize the encapsulation conditions for Nongmangkha flower extract using ionic gelation and to evaluate its physicochemical properties and bioaccessibility using *in vitro* gastrointestinal release behavior. Also, comprehensive set of characterization techniques including FTIR, SEM, and DSC was utilized to enhance the reliability of the encapsulation. This study is expected to further broaden the sphere of utilization of phytochemical-loaded encapsulates as potential delivery systems and formulation of functional foods with enhanced phytochemical protective properties.

5.2. Materials and Methods

5.2.1. Flower extract preparation

Nongmangkha flower extract was prepared by using novel extraction technique to obtained maximum total phenolic content than a conventional technique. Based on earlier study ultrasound pretreated microwave assisted extraction technique was adopted at 700 W for 5 min (Chapter 4). The sample-to-solvent (80 % ethanol) ratio was 1:10. Initially, the mixture was treated with ultrasound at 250 W for 15 min, followed by microwave-assisted extraction of phenolic compounds. Rotary evaporator (ROTEVA-8703, Equitron, India) was used to dry the obtained flower extract at 40 °C and kept at 4°Cuntil further use.

5.2.2. Encapsulation of flower extract by ion gelation

Ionic gelation technique was employed to encapsulate Nongmangkha flower extract (Patel et al., 2016). To investigate the influence of sodium alginate (SA) and calcium chloride ($CaCl_2$) concentrations on encapsulation efficiency, a central composite design (CCD), based on response surface methodology (RSM), was employed. CCD (Face centered) was selected because it allows for the development of a second-order polynomial model that captures both linear and quadratic effects, as well as interactions between independent variables. SA (1–3 %) and $CaCl_2$ (3–7 %) were selected as independent variables, while the encapsulation efficiency (EE) of total phenolic content (TPC) was taken as the response variable. A total of 13 experimental runs were carried out as part of the central composite design, including factorial points, axial points, and repeated center points to improve reliability. It also helps identify the best combination of variables for encapsulation while using fewer experiments and reducing possible errors.

During the optimization of the encapsulation process, the concentration of flower extract was fixed at 2 % (w/v) relative to the volume of the SA solution. Keeping the extract concentration constant helped maintain consistency across all experimental runs and avoided interference in the model's accuracy. Since the flower extract was the material being encapsulated, and not part of the gelling system, it was not included as a variable in the optimization design.

To prepare the SA solution, SA was mixed with deionized water at ~700 rpm and 28 ± 3 °C for 2 h until complete dissolution. The Nongmangkha flower extract was then added to the SA solution and mixed thoroughly until a homogeneous mixture was obtained. This mixture was loaded into a 3 mL syringe (23 gauge, metal needle) and carefully dropped into a $CaCl_2$ solution (cross-linking agent) from a needle-to-surface height of 10 cm, under continuous stirring at 700 rpm (at 27±3 °C). The required concentration of $CaCl_2$ solution was prepared by using deionized water. The resulting beads were allowed to remain in the $CaCl_2$ solution for 30 min to facilitate gelation and bead stabilization. The beads were recovered by filtration using Whatman No. 1 filter paper and rinsed thoroughly using deionized water to remove excess Ca^{2+} ions. The washed beads were placed on petri dishes, dried in a tray dryer, and stored in airtight containers for subsequent analyses.

Once the optimal encapsulation conditions were established, the ability of the optimized system to accommodate different levels of phenolic content was evaluated by varying the concentration of flower extract. Four formulations were prepared using 1 % (S1), 2 % (S2), 3 % (S3), and 4 % (S4) (w/v) of flower extract, relative to the volume of sodium alginate solution. A control sample (C) without flower extract was also prepared. This post-optimization step aimed to assess the extract-to-polymer ratio and its effects on physicochemical properties, loading efficiency, structural integrity, and the retention of phenolic compounds at increasing concentrations. A sequential design approach—first optimizing the encapsulation conditions, followed by evaluation of extract loading—is widely used in encapsulation studies to achieve a balance between formulation efficiency and practical feasibility (Zam et al., 2014).

5.2.3. Determination of moisture content in encapsulated beads

Initial weights of the prepared encapsulates were noted and hot-air dried at 105 °C; intermittent weight of encapsulates were taken until constant weight. Equation (5.1) was used to calculate the moisture content of encapsulates (Patel et al., 2016) and repeated in triplicates.

$$\text{Moisture content (\%)} = \frac{\text{Initial weight} - \text{Final weight}}{\text{Initial weight}} \times 100 \qquad (5.1.)$$

5.2.4. Total phenolic content (TPC) and Total flavonoid content (TFC) of encapsulates

According to the protocol from Arriola et al. (2019) the encapsulates were first mixed with 5 % sodium citrate solution to dissolve completely at 37 °C and filtered through using Whatman no. 1 filter paper. After that, TPC content of encapsulates were obtained by following Folin Ciocalteau assay (Pasukamonset et al., 2016) with modifications. In a test tube 0.2 mL flower extract was taken, 0.5 mL of Folin Ciocalteau reagent and 2 mL of sodium carbonate (Na_2CO_3) (20 %) were added. After 1 h incubation in dark room at room temperature, the absorbance was recorded at 750 nm on a UV-vis spectrophotometer. The experiment was performed in triplicates; gallic acid was used as a standard and the results were expressed as mgg^{-1} of gallic acid equivalents (GAE).

The TFC was measured using the aluminium chloride ($AlCl_3$) colorimetric method as described by Panhekar et al. (2019). To begin with, 1 mL of the sample extract was mixed with 4 mL of deionised water in a test tube. Following this, 0.3 mL of 5 % sodium nitrite solution was added and allowed to incubate for 5 min. Then, 0.3 mL of 10 % $AlCl_3$ solution was introduced, and the mixture was left to stand for another 5 min. Subsequently, 2 mL of 1 M sodium hydroxide was added, and the final volume was adjusted to 10 mL with deionized water. The resulting mixture was thoroughly mixed, and its absorbance was recorded at 510 nm using a spectrophotometer. A calibration curve was prepared using quercetin as the standard, and the flavonoid content was expressed as milligrams of quercetin equivalent per gram of extract (mg $QAEg^{-1}$) and the experiment for each sample were conducted in triplicates.

5.2.5. Determination of DPPH of encapsulated beads

For sample preparation, encapsulates were mixed with 5 % sodium citrate solution and allowed to dissolve completely at 37 °C and filtered by using Whatman no. 1 filter paper (Arriola et al., 2019). Antioxidant activity was assessed using a slightly modified version of the method described by Pasukamonset et al. (2016) and Tundis et al. (2015). 0.5 mL sample was mixed with 3 mL of 0.1 mM 2,2-diphenyl-1-picrylhydrazyl (DPPH) solution. After 30 min of incubation at room temperature, the absorbance was measured at 515 nm. The results were expressed as the percentage of DPPH radical inhibition. All samples were analysed in triplicates.

5.2.6. Swelling and solubility of encapsulates

Swelling of the encapsulates was measured following the method described by Sharma et al. (2022) and Patel et al. (2016). Briefly, 120 mg of encapsulates were immersed in 30 mL of deionized water and allowed to rest for 2 h to permit swelling. After incubation, the encapsulates were carefully removed, gently blotted to remove excess surface water, and weighed.

For solubility determination, 120 mg of encapsulates (total weight of encapsulates) were mixed with 30 mL of deionized water using a vortex mixer for 30 minutes to facilitate solubilization. The insoluble encapsulates were then removed, the remaining supernatant with soluble encapsulates was collected and dried in a hot air oven at 105 °C until a constant weight was achieved. This is the weight of dissolved

encapsulates. The swelling index and solubility (%) were calculated using Equations (5.2) and (5.3), respectively. All analysis was performed in triplicate

$$\text{Swelling index} = \frac{\text{final weightofbeads} - \text{initial weight of beads}}{\text{initial weight ofbeads}} \quad (5.2)$$

$$\text{Solubility} = \frac{\text{weight of dissolved encapsulates}}{\text{total weight of encapsulates}} \times 100 \quad (5.3)$$

5.2.7. Encapsulation efficiency

The EE was determined by using spectrophotometer (Carry 100, Agilent Technologies, USA) and the Folin Ciocalteu reagent (Sharma et al. 2022). To determine the surface phenolic content, the encapsulated flower extract was washed in ethanol for 5 min, vortex mixed for 15 s and then filtered through Whatman no. 1 filter paper. The filtrate was taken for analysis of surface TPC of encapsulates. Gallic acid equivalent (GAE) in milligram per gram of encapsulates was used to express the EE of total phenolic content and analysis were done in triplicates. Equation (5.4) was used to estimate EE.

$$\text{Encapsulation efficiency} = \frac{\text{TPC flower extract} - \text{Surface TPC}}{\text{TPC flower extract}} \times 100 \quad (5.4)$$

5.2.8. Color measurement

Color parameters of encapsulates i.e., L*, a*, and b* were detected by using a hunter colorimeter (Hunter Lab, Reston, Virginia, USA). The color readings were recorded in triplicates for the encapsulated flower extract.

5.2.9. Morphology

Microscopic structure of encapsulates were of encapsulates were executed with the help of scanning electron microscope (Model: JEOL JSM-6390LV, Tokyo, Japan) at 20 kV at 65X magnification. Encapsulated Nongmangkha flower were placed on stubs with platinum layering before SEM analysis. All the formulations of encapsulates were assessed for digital image analysis.

5.2.10. Fourier-transform infrared spectroscopy (FT-IR)

Encapsulated flower extract prepared by using sodium alginate and calcium chloride were subjected to FT-IR spectroscopic analysis. Each encapsulates was grinded

in morter- pastel before proceeding to FT-IR analysis. These crushed encapsulates were mixed with potassium bromide and dried before compressed to form disc. FT-IR spectra of the encapsulated beads were recorded and under a wavenumber range of 400 to 4000 cm^{-1}.

5.2.11. Differential Scanning Calorimetry (DSC)

The thermal behavior of encapsulated flower extract was analysed by using differential scanning calorimetry (DSC 214 NETZSCH, Germany). DSC detection was performed, where the sample of 10mg was sealed in aluminum DSC pan. Temperature range of -20 °C to 300 °C was set for heating the pan and the flow rate was 10 °C min^{-1} in inert stream atmosphere at 50 ml min^{-1} of nitrogen (Belščak-Cvitanović et al., 2016). The phase properties of Nongmangkha flower extract encapsulates were represented by differential scanning calorimetry thermogram using NETZSCH Proteus software program (NETZSCH, Germany).

5.2.12. *In vitro* digestion of encapsulates and its release kinetics of polyphenols

The study involved the evaluation of encapsulated Nongmangkha flower extract compared with crude flower extract under controlled conditions to simulate digestion processes. Optimized encapsulated Nongmangkha flower extract and crude flower extracts were dissolved in deionized water separately. The digestion process followed the INFOGEST 2.0 static *in vitro* digestion protocol, ensuring consistency and reproducibility (Butterworth et al., 2012). Briefly, for oral phase, each sample (beads and flower extract) was added into simulated salivary fluid (SSF) containing salivary amylase in 1:1 ratio by weight. The mixture was incubated at 37 °C (5 min). For gastric phase, the resulting oral bolus was introduced into simulated gastric fluid (SGF) in 1:1 ratio by volume. Pepsin and gastric lipase were added, and the mixture was incubated for 2 h (at 37 °C, pH 3 maintained). For intestinal phase, the gastric chyme was further mixed with simulated intestinal fluid (SIF) in a 1:1 ratio by volume. Pancreatic enzymes and bile salts were added (maintaining at pH 7). The mixture was incubated at 37 °C (2 h). Additionally, control (blank) was prepared, enzymes added without samples to assess stability in digestive fluids. Following digestion, samples were centrifuged at 5000 rpm for 15 min and supernatants were collected at each phase (oral, gastric, and intestinal) for compositional analysis.

Release kinetics of polyphenols after *in vitro* digestion of encapsulates was measured using a modified Guggenheim approach where the intervals between measurements are not constant and the log of slope method as described previously (Borah et al., 2019). In brief, a first-order equation that describes digestibility of starch is shown in Eq. 5.5,

$$C_t = C_\infty (1 - e^{-kt}) \quad (5.5)$$

where C_t is the product concentration at time t, C_∞ is the end-point product concentration and k is the first-order rate constant of digestion. Eq. (5.5) could be further arranged as,

$$ln\left(\frac{dc}{dt}\right) = ln\,(C_\infty k) - kt \quad (5.6)$$

Therefore, Eq. (5.6) represents a linear relationship of $ln\left(\frac{dc}{dt}\right)$ plotted against time t with a slope of $-k$, where $ln\,(C_\infty k)$ is the y-intercept and the value of k can be estimated from the plot. This is the logarithm of the slope (LOS) plot.

TPC released from the encapsulates into the simulated intestinal fluid were monitored using UV-Vis spectroscopy for release kinetics and bioaccessibility studies observed at random time intervals such as 5, 10, 20, 30, 60, 90 and 120 min. Additionally, TPC data obtained from *in vitro* digestion of crude flower extract without encapsulation were used as comparators to assess polyphenol degradation by gastric pH. It may be noted that crude flower extract was chosen as a comparator and the measurement of its TPC release kinetics is not an assessment of its control release properties but solely for the purpose of comparison.

5.2.13. Statistical analysis

All experiments were conducted in triplicate, and results are expressed as mean ± standard deviation (SD). In addition, 95 % confidence intervals (CIs) were calculated to provide an estimate of the precision around the mean values. One-way analysis of variance (ANOVA) followed by Duncan's post-hoc test was used to determine significant differences between groups at $p < 0.05$. Statistical analysis was performed using SPSS software (SPSS, USA), while graphs for FT-IR, DSC, and related analyses were generated using Origin software (2018, Windows version).

5.3. Results and Discussion

5.3.1. Model fitting for encapsulation efficiency (EE)

Central composite design (CCD) based response surface methodology was used to obtain the optimized condition for the ionic gelation technique using SA and $CaCl_2$. Here, 13 experimental runs were performed to understand the effect of SA and $CaCl_2$ on encapsulation efficiency of TPC. All experimental runs with results are shown in Table 5.1. Quadratic model was selected in this experimental design and ANOVA was employed to analyze the impact of different variables and to identify the model statistical validity with 0.05 significance levels.

5.3.2. Influence of Variables on EE

ANOVA for EE is summarized in Table 5.2. An F-value of 24.16 and a p-value of 0.0003 indicated that the model was statistically significant and well fitted. Among factors, sodium alginate concentration (A) exhibited the highest influence ($F = 89.31$, $p < 0.0001$), while calcium chloride concentration (B) had a marginally significant effect ($F = 5.41$, $p = 0.0530$). Interaction between factors A and B ($F = 1.77$, $p = 0.2250$) was not significant and the quadratic components A^2 and B^2 were statistically significant, with respective p-values of 0.0494 and 0.0175.

The coefficient of determination (R^2) of the developed quadratic model was 0.72, indicating that 72 % of the variability in EE could be explained by the selected independent variables i.e., SA and $CaCl_2$ concentrations. While this reflects a reasonably good model fit for a biological system, it also implies that 28 % of the variability may be attributed to other unaccounted factors such as minor experimental fluctuations, environmental conditions (e.g., humidity or temperature during bead formation), or inherent batch-to-batch variability in the extract composition etc. Furthermore, the non-significant lack-of-fit ($p = 0.1065$) and significant model F-value ($F = 24.16$, $p = 0.0003$) confirmed the adequacy of the model within the design space. The adjusted R^2 value was a bit lower, but it still showed that the model was reliable in explaining the data. Because the lack-of-fit isn't statistically significant ($F = 4.01$, $p = 0.1065$), it shows the model works well for predicting results within the design space. The residuals are minimal, supporting the model's reliability. The significant quadratic terms (A^2 and B^2) highlight the non-linear behavior of the system, underscoring the importance of optimal

concentrations. Additionally, the relatively high F-value for sodium alginate demonstrates its dominant effect on encapsulation efficiency compared to calcium chloride. Moreover, the inclusion of center points helped to estimate pure error and test model curvature, supporting the robustness of the model structure. Thus, CCD proved to be a statistically sound approach for optimizing the encapsulation process, enabling both accurate response prediction and efficient experimental design.

The polynomial model Equation (5.7) is resulted:

$$EE = 64.70 + 10.37\,A - 2.55B \quad (5.7)$$

Where, EE is the encapsulation efficiency (%), A is the concentration of sodium alginate (%) and B is the concentration of calcium chloride (%).

The model coefficients suggest that a higher concentration of SA substantially improves encapsulation efficiency, whereas $CaCl_2$ has a smaller, negative linear effect. This observation is consistent with the underlying gelation mechanism of alginate, where excessive Ca^{2+} ions can create an overly dense and rigid network structure, which may impede the effective entrapment of phenolic compounds.

The results demonstrate that SA concentration is a critical factor influencing the encapsulation efficiency of TPC, consistent with its role in forming a stable ion-gel matrix. Calcium chloride's moderate impact suggests its importance in cross-linking efficiency, particularly at intermediate concentrations. The lack of significant interaction effects indicates that SA and $CaCl_2$ independently contribute to encapsulation. Quadratic terms suggest non-linear effects, highlighting the importance of optimizing concentrations for maximal efficiency. The response surface methodology effectively optimized the process, providing a predictive model for encapsulation efficiency with strong statistical validity.

It was seen that at 3 % SA the polymer chains are sufficiently concentrated to form a stronger gel network when cross-linked with $CaCl_2$. This improves the better trapping the phenolic compounds within the beads. Excess $CaCl_2$ leads to formation of a denser and more rigid network. Indeed, over cross linking makes the network too rigid becomes less permeable, preventing the flower extract's phenolic compounds from being effectively trapped (Ching et al. 2017 and Pasukamonset et al. 2016). At 5 % $CaCl_2$, $Ca2^+$ ions are available to form a stable gel network without causing excess precipitation

and rigidity. Also, excess $CaCl_2$ reduced the porosity of the beads, making it harder for the encapsulated phenolic compounds to diffuse into the gel network, leading top lower encapsulation efficiency.

The response surface plot (Fig.5.1) illustrated the influence of SA and $CaCl_2$ concentrations on the encapsulation efficiency of TPC. SA concentration had a significant positive effect, with higher concentrations yielding improved efficiency. $CaCl_2$ effect was less pronounced, with moderate levels (5 %) optimizing encapsulation.

5.3.3. Optimized condition

The optimized condition was obtained in the software (Design Expert) by selecting the independent variables such as SA and $CaCl_2$ in range and maximizing the EE. Here, numerical optimization technique was used. The optimized conditions for maximum encapsulation efficiency were identified as 3 % SA and 5 % $CaCl_2$, predicting an EE of 75.72 % with desirability of 1.00. Experimental validation yielded an efficiency of 72.19±5.19 %, closely aligning with the predicted value and confirming the model's reliability.

Table 5.1. Experimental runs with response data of various encapsulated flower extract

Run no.	Sodium Alginate (%)	Calcium Chloride (%)	Encapsulation Efficiency (%)
1	1	3	56.13
2	1	5	52.9
3	1	7	47.25
4	2	3	64.42
5	2	5	69.44
6	2	5	68.63
7	2	5	73.16
8	2	5	70.51
9	2	5	71.51
10	2	7	59.73
11	3	3	73.31
12	3	5	73.58
13	3	7	71.58

Table 5.2. ANOVA for ionic gelation of encapsulation efficiency of TPC

Source	df	Sum of Squares	F-value	p-value
Model	5	174.40	24.16	0.0003
A-sodium alginate	1	644.60	89.31	<0.0001
B- Calcium chloride	1	39.01	5.41	0.053
AB	1	12.78	1.77	0.225
A^2	1	40.65	5.63	0.0494
B^2	1	69.09	9.57	0.0175
Residual	7	7.22		
Lack of Fit	3	12.64	4.01	0.1065
Pure Error	4	3.15		
Cor Total	12			
R^2	0.72			
Adjusted R^2	0.906			
Predicted R^2	0.699			

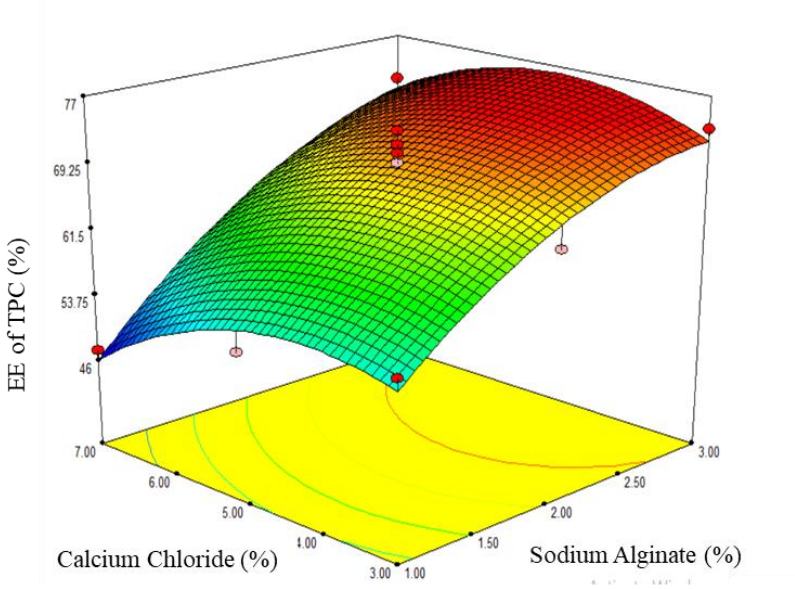

Fig. 5.1. Response surfaces for encapsulation efficiency of total phenolic content

5.3.4. Properties of encapsulated flower extract made with varying concentration of flower extract

5.3.4.1. Moisture content

The presence of moisture affects key properties such as density, flowability, hygroscopic nature, caking, and shelf life. The moisture of encapsulates of flower extract ranges from 95.33 to 95.54 % (Table 5.3). Statistically, there was significant difference of moisture content among S1, S2, S3 and S4.

5.3.4.2. TPC, TFC, EE and DPPH radical scavenging activity

TPC was observed to be in the range of 3.63 to 13.23 mg GAE/g. A significant difference ($p < 0.05$) in TPC was observed among the samples, except between S3 and S4, where no statistically significant difference was found. Increasing the flower extract also increases the TPC content in encapsulated flower extract. This retention is attributed to the protective barrier provided by the sodium alginate matrix, which effectively shielded the bioactive compounds from degradation during storage and digestion.

Encapsulation efficiency of TPC was found to have a significant difference ($p < 0.05$) between S1 and other formulations. S3 and S4 showed the highest encapsulation efficiency (shown in Table 5.3), S3 (72.01 %) and S4 (74.05 %) showed no significant difference. These results demonstrated that by increasing the sample concentration, the encapsulation efficiency of encapsulated flower extract could be increased. It was also noted that phenolic compounds leach out into the calcium chloride solution, which may have contributed to a reduction in encapsulation efficiency. This may be attributed to the alginate solution encountering the calcium chloride solution through its porous structure, which results from the presence of low molecular weight compounds in the polymer (Tzatsi et al., 2021). Additionally, reduced diffusion into the external aqueous medium at higher extract concentrations during the fixed curing period could have led to increased encapsulation efficiency (Zam et al., 2014). It was reported that encapsulation efficiency in *Clitoria ternatea* petal flower ranged from 74.97 to 84.83 % (Pasukamonset et al., 2016). Total flavonoid content was observed to have significant difference among encapsulates ranging from 0.29 (S1) to 1.25 (S4) (mg QE g^{-1}). Significant difference was seen in the DPPH radical scavenging activity of encapsulated

flower extract, higher sample concentrations in the encapsulation formulations led to an increase in DPPH radical scavenging activity. Antioxidant activity also increased from S1 to S4 as flower extract concentration increased, S4 showed the highest antioxidant activity, 75.79 %.

5.3.4.3. Swelling ratio and Solubility

The results of swelling and solubility of encapsulates viz. S1, S2, S3 & S4 are illustrated in Table 5.3. No statistically significant difference ($p < 0.05$) was observed among S1, S2, S3, and S4. The variation of weight of samples could influence the swelling. The swelling ratio ranged from 0.15 to 0.16, S3 encapsulates had higher swelling index.

The solubility ranged from 136.38 to 136.57 % (Table 5.3) and there was no significant difference among encapsulates (S1, S2, S3 and S4). The encapsulates were of uniform size and since solubility is affected by size and surface area, there was no significant difference in solubility. However, solubility of encapsulates resulted from the hydrophilicity of sodium alginate (presence of ionised carboxylic group) and the dissolution of flower extract (Carvalho Tavares et al., 2016).

Table 5.3. Physicochemical properties of encapsulated flower extract

Sample / Properties	**S1**	**S2**	**S3**	**S4**
Moisture (% wet basis)	95.33±1.100^{a}	95.38±1.16^{a}	94.72±0.63^{a}	95.54±1.405^{a}
TPC (mg GAE/g)	3.63±0.525^{a}	8.29±0.978^{b}	12.13±0.987^{c}	13.23±0.368^{c}
TFC (mg QAE/g)	0.29±0.051^{a}	0.66±0.140^{b}	1.15±0.115^{c}	1.25±0.184^{c}
DPPH (% RSA)	48.69±0.717^{a}	71.54±0.877^{b}	73.63±1.340^{c}	75.79±0.546^{c}
Encapsulation efficiency (%)	42.59±1.817^{a}	70.20±1.030^{b}	72.02±1.822^{cd}	74.05±0.901^{d}
Solubility (%)	136.38±0.58^{a}	136.57±0.38^{a}	136.32±0.262^{a}	136.37±0.231^{a}
Swelling index	0.15±0.012^{a}	0.15±0.006^{a}	0.14±0.008^{a}	0.16±0.006^{b}

All values are expressed as the mean ± SD of three replicates. Means with different letters in each row are significantly different ($p \leq 0.05$).

5.3.4.4. Color measurement of encapsulated flower extract

Color parameters indicated the retention of flower extract or the bioactive compounds in the encapsulated flower extract. The color values of all the formulations (S1, S2, S3 & S4) of encapsulated flower extract are shown in Table 5.4. All encapsulated flower extract indicated redness (a^*) and yellow (b^*) color values. A trend could be seen that higher concentration of flower extract provided higher color parameters of encapsulated flower extract.

Table 5.4. Color parameters of encapsulates of flower extract

Parameters	Control	S1	S2	S3	S4
L	61.593 ±0.513^{e}	56.657 ±0.317^{d}	53.627 ±0.261^{c}	51.21 ±0.261^{b}	49.977 ±0.748^{a}
a*	-1133 ±0.131^{a}	3.85 ±0.046^{b}	6.320 ±0.122^{d}	6.137 ±0.0416^{c}	7.193 ±0.086^{e}
b*	8.47 ±0.056^{a}	26.44 ±0.142^{d}	29.82 ±0.438^{e}	25.327 ±0.189^{b}	26.01 ±0.118^{c}

All values are expressed as the mean ± SD of three replicates. Means with different letters in each row are significantly different ($p \leq 0.05$).

5.3.4.5. Scanning electron microscope (SEM)

All the formulations of encapsulated flower extracts were selected for SEM studies. SEM micrographs analysis revealed smooth, oval shape beads with uniform size, indicative of effective encapsulation. The surface morphology of sodium alginate encapsulated follower extract is shown in Fig.5.2. It was observed that the control encapsulates without flower extract had a rough, collapsed, shriveled shape with cracks appearing on the surface after drying. But the dried encapsulated flower extract were found to have a smoother surface than the control beads. The flower extract might have reduced porosity of the polymer matrix by filling in gaps between the polymer networks. Such morphology of alginate matrix provides a robust barrier against environmental stress and aids in the controlled release of bioactive compounds. However, cracks were observed in some of the encapsulated extract, which may have resulted from the partial collapse of the polymer network due to dehydration and could lead to the degradation or leakage of phenolic compounds from the encapsulated flower extract (Mandal et al. 2010).

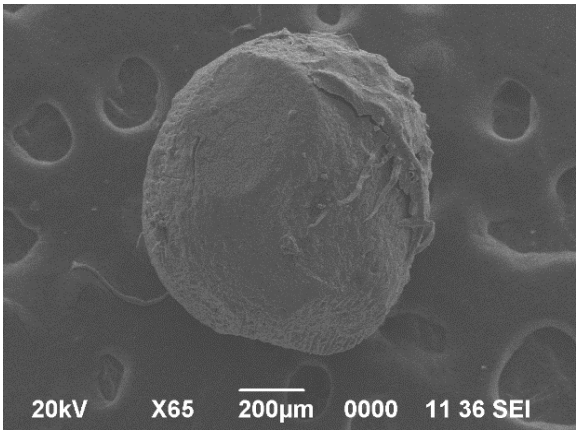

3 % sodium alginate, 5 % Calcium (Control)

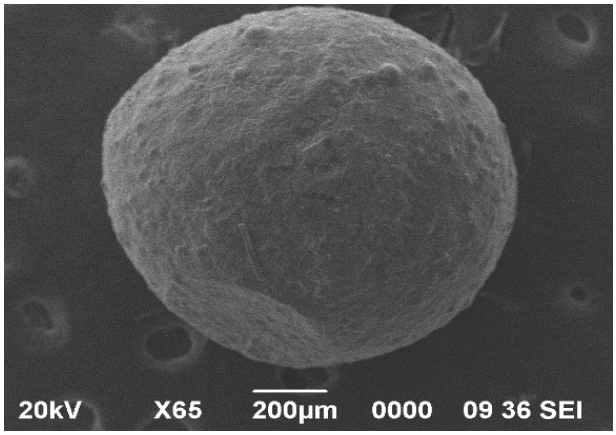

3 % sodium alginate, 5 % Calcium chloride (Optimized bead)

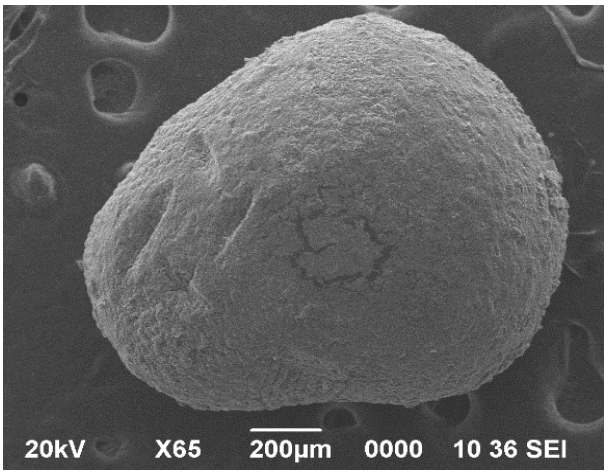

2%sodium alginate, 7% Calcium chloride

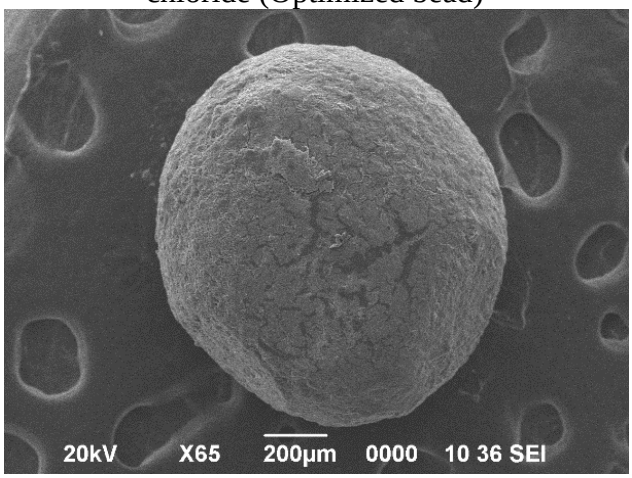

3%sodium alginate, 7% Calcium chloride

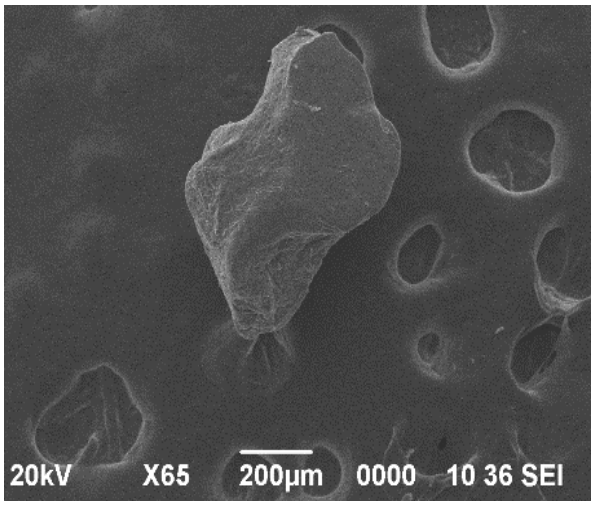

1% sodium alginate 7% calcium chloride

Fig. 5.2. SEM images of encapsulates of flower extract

Among the four formulations (S1–S4), S4 exhibited slightly higher encapsulation efficiency and antioxidant activity compared to S3. However, S3 was selected as the optimized formulation due to a more favorable balance between encapsulation performance, bead integrity, and practical formulation considerations. Specifically, S3 (3 % extract) showed high encapsulation efficiency (74.05 %), strong antioxidant activity, and uniform bead morphology, while maintaining better structural stability during drying and handling. Moreover, from a formulation and cost efficiency perspective, S3 offers a more practical solution, reducing raw material usage while maintaining excellent functional and physicochemical properties. Therefore, S3 was chosen as the most balanced and scalable formulation for future application.

5.3.4.6. FTIR analysis

FTIR spectra (Figure 5.3) confirmed the successful encapsulation of flower extract by showing characteristic kinks corresponding to functional groups i.e, carboxylic (-COOH), hydroxyl (-OH), and amino (-NH) groups. These kinks were prominent in the encapsulated beads, indicating interactions between the alginate matrix and bioactive compounds. These distinct bands confirmed the presence of phenolic compounds in the flower extract and suggested strong interactions between the alginate matrix and the encapsulated bioactives. This structural stability supports the retention of phenolic and flavonoid in the encapsulated form. Broadkinks at 3200–3400 cm^{-1} corresponds to the O-H stretching of hydroxyl groups, indicative of phenolic compounds; kinks at 1635 cm^{-1} and 1545 cm^{-1} represent stretching of C=O and N-H bending, respectively, confirming carboxylic acids and amino groups presence and vibrations at 1250–1300 cm^{-1} signify C-O stretching in aromatic rings, consistent with phenolic structures. The spectrum of control bead lacked the distinctive kinks of the flower extract, such as those at 3200–3400 cm^{-1} and 1635 cm^{-1}**,** confirming that the above observed kinks in the encapsulated flower extract were due to the phenolics or other bioactive compounds from the flower extract. So, it was observed that hydrogen bonding and ionic interactions provided structural stability, enhancing the retention of phenolic compounds during storage and digestion. Encapsulation reduced the intensity of kinks associated with free hydroxyl and carbonyl groups, indicating that these functional groups were involved in bonding with the matrix.

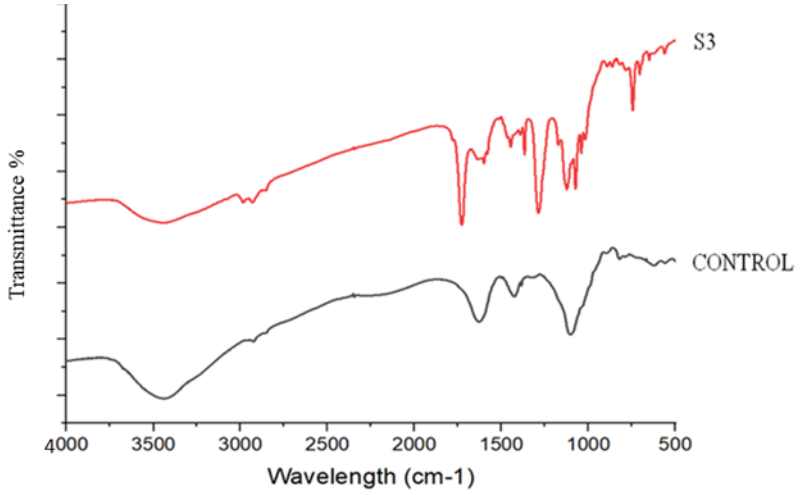

Fig. 5.3. FTIR spectra of encapsulated flower extract and control

5.3.4.7. Thermal Properties of encapsulates

The thermal behavior of the encapsulated flower extract was evaluated using differential scanning calorimetry (DSC), and the results are presented in Table 5.5. Two distinct endothermic peaks were observed in all samples, indicating thermal transitions associated with the phenolic compounds and polymer matrix. Peak 1 observed in the range from 40.8 – 60.3 °C to 104 – 118 °C, this transition might be related to the loss of low-molecular-weight volatile compounds. Among them, S3 exhibited the lowest onset (40.8 °C) and peak temperature (77.3 °C)**,** possibly due to interaction between phenolic compounds and alginate matrix, which is also supported by highest EE % of S3, as shown in Table 3. Peak 2 (186.3–20.6 °C) is attributed to the melting or degradation of higher molecular weight phenolic compounds or alginate network transitions.

Table 5.5. Differential scanning calorimetry (DSC) study of encapsulated flower extract

	Peak 1				Peak 2			
Sample	**Temperature**	**range**	**Peak**	**Area**	**Temperature**	**range**	**Peak**	**Area**
	T_o (°C)	**T_e(°C)**	**T_p(°C)**	**(ΔH_m)**	**T_o (°C)**	**T_e(°C)**	**T_p(°C)**	**(ΔH_m)**
Control	60.3	114.3	92.4	430.2	186.3	206.7	195.7	93.89
S1	50.1	118.0	88.4	263.3	195.4	208.3	199.2	93.2
S2	47.6	112.7	85.8	336.6	189.9	208.9	196.7	101.6
S3	40.8	104.7	77.3	302.6	193.8	209.6	201.3	65.55
S4	55.5	118.0	92.4	354.5	188.9	208.5	195.0	99.07

5.3.4.7. *In vitro* release of total phenolic compounds

The *in vitro* digestion results demonstrated a controlled release of phenolic compounds from encapsulates at the intestinal phase. For encapsulates as shown in Fig. 5.4, the release of phenolic compounds was recorded the highest during the intestinal phase compared to the oral and gastric phases. Overall, the TPC detected in the digestion fluid for the encapsulates were higher than that of the crude extract in all three phases of digestion (oral, gastric and intestinal). Note that the TPC detected here for crude extract is not a release mechanism but a comparative demonstration of how TPC values fluctuate/degrade with change in pH during the simulated digestion process when not protected inside a polymer matrix via encapsulation.

Digestion kinetics of released phenolic compounds at the intestinal phase revealed that two distinct phases with different rate constants (k_1 and k_2) appeared for the encapsulates whereas a single phase dominated for crude extract. The encapsulates exhibited a biphasic release pattern, with an initial rapid release (phase1) followed by a slower, sustained release phase (phase2) illustrated in Fig. 5.5A. Phase1 visibly showed the rapid release of phenolic content which was characterized by rate constant k_1= 0.12 min^{-1} and a concentration C_{t1}= 0.019 $mgmL^{-1}$(Table 5.6). This phase likely represents the immediate diffusion of loosely bound phenolic from the outer periphery of the encapsulates. In phase2, a slower secondary release phase with k_2= 0.021 min^{-1} and at concentration C_{t2}= 0.02 $mgmL^{-1}$ was observed (Table 5.6). This phase suggests a controlled or sustained release due to diffusion from the inner regions of the encapsulates. Digestion kinetics of crude extract (Fig. 5.5B) revealed only a single phase1 (k_1= 0.014 min^{-1}, C_{t1}= 0.016 $mgmL^{-1}$). The absence of phase2 indicated that the phenolic compounds from the crude extract become immediately available in absence of a protective barrier, rather than a sustained release overtime as with the case of encapsulates with two distinct phases.

Release kinetics analysis indicated that the encapsulate provided better control over the encapsulated polyphenolic compounds release compared to the performance of the crude extract, which exhibited no release pattern. The protective nature of the encapsulation matrix was evident in the gastric phase, phenolic release occurred lower comparatively to other phases, highlighting the resistance of the encapsulates to acidic

environments. This resistance is critical for supporting the delivery of bioactive compounds to the intestinal phase, where their absorption and bioavailability are maximized. Compared to the crude flower extract, the encapsulates showed superior stability and exhibited a controlled release pattern. The crude extract demonstrated a higher rate of degradation during the gastric phase, leading to lower phenolic content reaching the intestinal phase (Fig. 5.5). The encapsulation matrix effectively mitigated these losses, enhancing potential bioavailability of phenolic compounds in the target phase. Release kinetics followed a biphasic pattern, with an initial rapid release (phase1) followed by a slower, sustained release (phase2). Encapsulation effectively mitigated the premature release of phenolics in the gastric phase, enhancing their availability in the intestinal phase, where absorption is maximized. The crude flower extract displayed no protective ability and immediate availability (no controlled release pattern) during digestion, resulting in a lower bioavailability of phenolic content in the intestinal phase. Encapsulates, on the other hand, protected phenolic content during the gastric phase and released them steadily in the intestinal phase, highlighting the superiority of encapsulation in preserving and delivering phenolic compounds.

Fig.5.4 shows the phenolic compounds released from the encapsulates were lesser during the oral and gastric phase, followed by increased release in the intestinal phase indicating resistance to acidic conditions and protection during the gastric digestion. The intestinal release kinetics showed rapid release during the initial phase (phase1), followed by a slower, sustained release in phase2 (Fig.5.5). The rate constants k_1 (initial rapid release) and k_2 (sustained release) indicated that the encapsulates provide an effective mechanism for controlled phenolic release. In contrast, the crude flower extract exhibited a rapid and unregulated release of phenolic compound, with significant degradation during the gastric phase. This highlights the protective and controlled release advantages of the encapsulated Nongmangkha flower extract. The findings are in agreement with earlier reports that the protection may be attributed to alginate, which helped preserve the phenolic compounds in the simulated gastric environment and enabled their controlled release afterward (Pasukamonset et al. 2016). However, these *in vitro* conditions are only a proxy measure which may not fully reflect *in vivo* conditions and will be the focus of future studies.

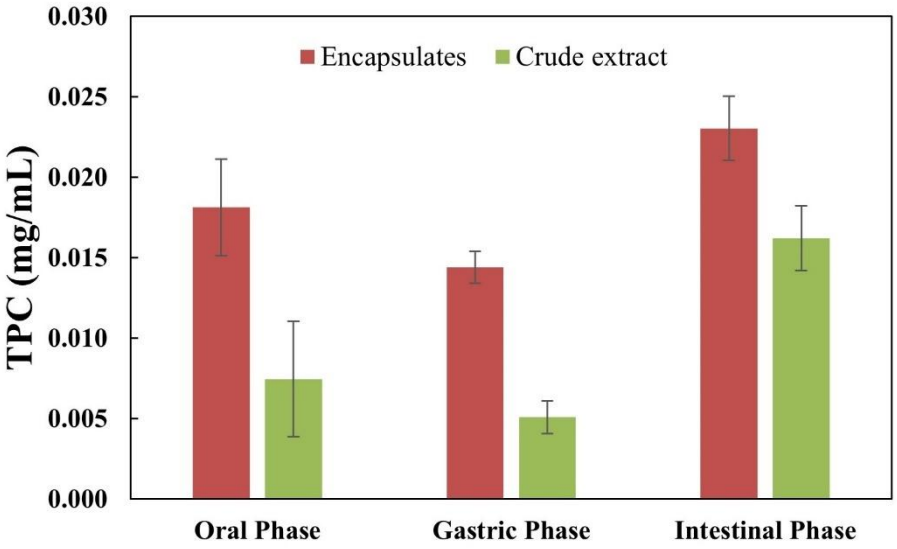

Fig. 5.4. *In vitro* digestion of encapsulates (S3) and crude extract, (■) and (■) indicate the TPC data detected in simulated fluids from oral, gastric and intestinal phases after digestion of encapsulates and crude extract.

Table 5.6. Release kinetics of total phenolic compound from the encapsulates of flower extract

		Encapsulates	**Crude extract**
Phase1	k_1 (min^{-1})	0.12	0.014
	C_{t1} (mg/mL)	0.019	0.016
Phase2	k_2 (min-^{1})	0.021	ND
	C_{t2} (mg/mL)	0.02	ND

where, $k_1$and k_2 (k_1>>k_2) represent first-order rate constants (min^{-1}) of *phase1* and *phase2*; C_{t1} and C_{t2} represent the amount of total phenolic compounds released (mg/mL) at *phase1* and *phase2* during in vitro digestion (intestinal phase). ND = Not detected

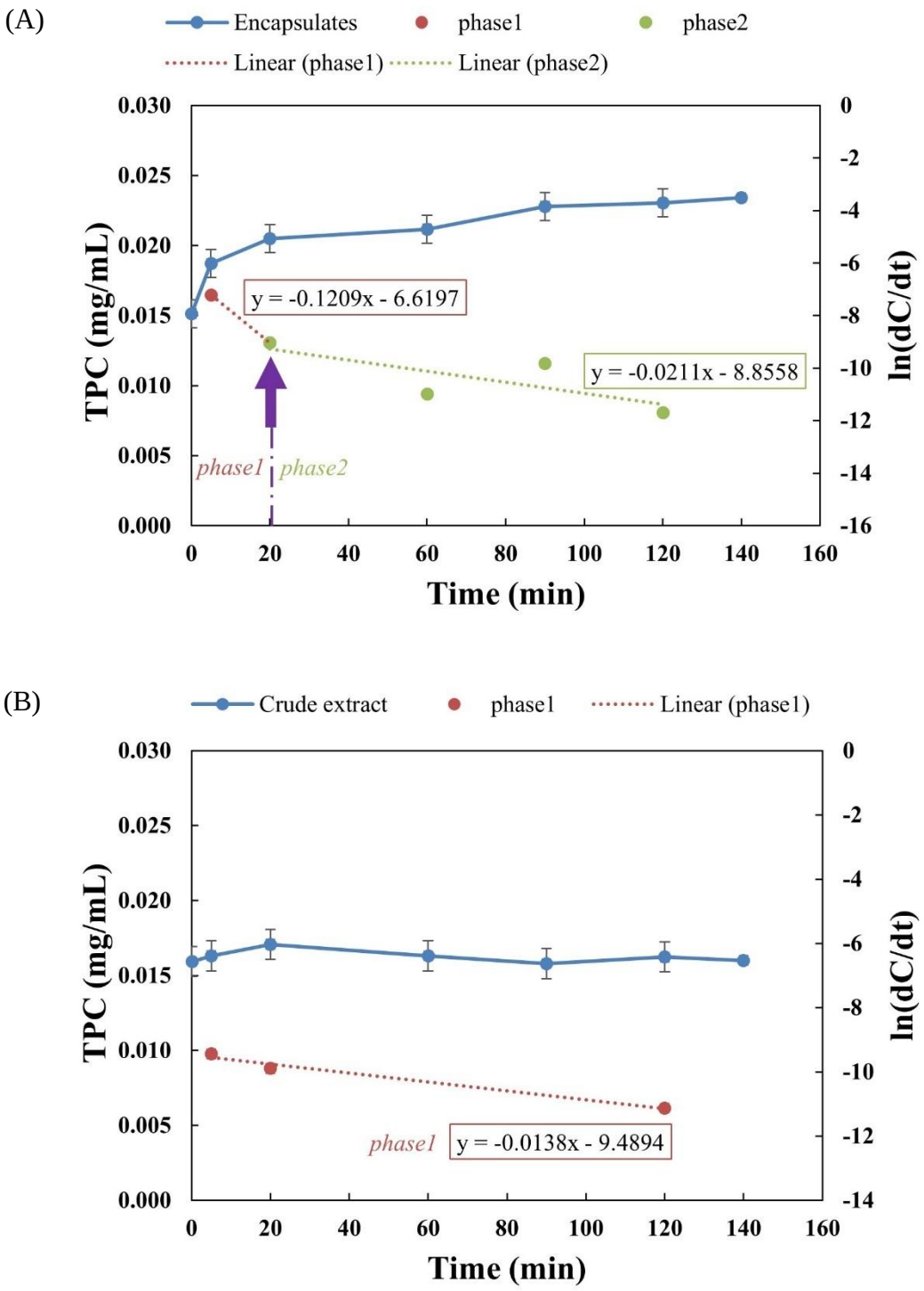

Fig. 5.5. Intestinal release kinetics of total phenolic compound from (A) encapsulates (S3) and (B) crude extract. Here, (●) indicates the TPC data detected at intermittent time intervals in simulated fluids from intestinal phase after digestion of encapsulates and crude extract; (●) and (●) represent the log of slope plot for phase1 and phase2 respectively.

5.5. Conclusions

This study demonstrates the potential of alginate-based ionic gelation for the encapsulation of Nongmangkha flower extract, offering improved retention of phenolic compounds and a controlled release profile under simulated oral-gastrointestinal conditions. The application of MAE followed by encapsulation via ionic gelation provides a dual strategy, not only enhancing extraction efficiency from Nongmangkha but also protecting the sensitive bioactive compounds during digestion and storage. The central composite design offered a statistically rigorous and efficient approach for modeling and optimizing the encapsulation process, yielding a reliable predictive model with good fit and minimal experimental error. The optimized formulation (3 % sodium alginate and 5 % calcium chloride) achieved high encapsulation efficiency and exhibited a biphasic release pattern, suggesting enhanced protective and delivery capabilities of the encapsulation matrix. While S3 showed a controlled and biphasic release profile, a portion of phenolics was still released during the gastric phase, indicating partial early leakage. This suggests that complete protection in acidic conditions may be limited and could be improved by further optimizing bead crosslinking or wall thickness. Our results suggest that the encapsulated Nongmangkha extract could be potentially used in making antioxidant-enriched functional foods like drinks, gummies, or health supplements, its slow release and better stability could deliver beneficial plant compounds effectively. Despite the promising results, this study has several limitations typical of early-stage food formulation research. The encapsulation and release studies were conducted under controlled laboratory conditions using *in vitro* oral-gastrointestinal models, which may not fully reflect the complexity of real food systems or physiological environments. The interaction of encapsulated compounds with other food ingredients, processing conditions (e.g., heating, homogenization, pH variation), and storage factors (e.g., humidity, light, temperature) were not evaluated and remains a topic of future investigations. Additionally, the bioaccessibility and bioavailability of the encapsulated phenolics were not assessed *in vivo*, and sensory characteristics were not examined, which are essential for consumer acceptance and industrial application. Further studies involving real food matrices, processing stability, storage behavior, and biological validation are needed to translate these findings into practical functional food or nutraceutical applications.

References

Ahmed, R., Sultana, T., Routary, R., Khan, S. H., & Shaari, K. (2016). Chemistry and antidiabetic effects of *Phlogocanthus thyrsiflorus Nees* flowers. *Natural Products Chemistry and Research*, 4(229), 2.

Arriola, N. D. A., Chater, P. I., Wilcox, M., Lucini, L., Rocchetti, G., Dalmina, M., Pearson, J. P., & Amboni, R. D. D. M. C. (2019). Encapsulation of stevia rebaudiana Bertoni aqueous crude extracts by ionic gelation–Effects of alginate blends and gelling solutions on the polyphenolic profile. *Food Chemistry*, *275*, 123-134

Bagherian, H., Ashtiani, F. Z., Fouladitajar, A., & Mohtashamy, M. (2011). Comparisons between conventional, microwave-and ultrasound-assisted methods for extraction of pectin from grapefruit. *Chemical engineering and processing: Process Intensification*, *50*(11-12), 1237-1243.

Borah, P. K., Rappolt, M., Duary, R. K., & Sarkar, A. (2019). Structurally induced modulation of in vitro digestibility of amylopectin corn starch upon esterification with folic acid. *International Journal of Biological Macromolecules*, *129*, 361-369.

Butterworth, P. J., Warren, F. J., Grassby, T., Patel, H., & Ellis, P. R. (2012). Analysis of starch amylolysis using plots for first-order kinetics. *Carbohydrate Polymers*, *87*(3), 2189-2197.

Ching, S. H., Bansal, N., & Bhandari, B. (2017). Alginate gel particles–A review of production techniques and physical properties. *Critical Reviews in Food Science and Nutrition*, *57*(6), 1133-1152.

Das, P., Kumar, K., Nambiraj, A., Rajan, R., Awasthi, R., &Dua, K. (2017). Potential therapeutic activity of *Phlogacanthus thyrsiformis Hardow (Mabb)* flower extract and its biofabricated silver nanoparticles against chemically induced urolithiasis in male Wistar rats. *International Journal of Biological Macromolecules*, *103*, 621-629.

de Carvalho Tavares, I. M., Lago-Vanzela, E. S., Rebello, L. P. G., Ramos, A. M., Gomez-Alonso, S., Garcia-Romero, E., & Hermosin-Gutierrez, I. (2016).Comprehensive study of the phenolic composition of the edible parts of jambolan fruit (*Syzygiumcumini (L.)Skeels*). *Food Research International*, *82*, 1-13.

George, M., & Abraham, T. E. (2006). Polyionic hydrocolloids for the intestinal delivery of protein drugs: alginate and chitosan—a review. *Journal of Controlled Release*, *114*(1), 1-14.

Grant, G. T., Morris, E. R., Rees, D. A., Smith, P. J., & Thom, D. (1973). Biological interactions between polysaccharides and divalent cations: the egg-box model. *FEBS Letters*, *32*(1), 195-198.

Izadifar, Z. (2013). Ultrasound pretreatment of wheat dried distiller's grain (DDG) for extraction of phenolic compounds. Ultrasonics Sonochemistry, 20(6), 1359–136.

Koushik, N., Zaman, M. K., & Saikia, K. (2020). Evaluation of anti-diabetic efficacy of the leaves and flower of *Phlogacanthus thyrsiflorus Nees*. *Journal of Pharmacognosy and Phytochemistry*, *9*, 979-982.

Kurozawa, L. E., & Hubinger, M. D. (2017). Hydrophilic food compounds encapsulation by ionic gelation. *Current Opinion in Food Science*, *15*, 50-55.

Mandal, S., Kumar, S. S., Krishnamoorthy, B., & Basu, S. K. (2010). Development and evaluation of calcium alginate beads prepared by sequential and simultaneous methods. *Brazilian Journal of Pharmaceutical Sciences*, 46, 785-793.

Nongthombam, I., Das, P., & Devi, J. (2018a). Evaluation of antioxidant activity of *Phlogacanthus thyrsiflorus Nees*: A medicinal plant. *Journal of Medicinal Plants Studies*, 6, 242-4.

Nongthombam, I., Das, P., & Devi, J. (2018b). Preliminary phytochemical screening of *Phlogacanthus thyrsiflorus Nees*: A medicinal plant. *Journal of Pharmacognosy and Phytochemistry*, 7(6), 1156-1158.

Pananun, T., Montalbo-Lomboy, M., Noomhorm, A., Grewell, D., & Lamsal, B. (2012). High-power ultrasonication-assisted extraction of soybean isoflavones and effect of toasting. LWT-Food Science and Technology, 47(1), 199–207.

Panhekar, D., Sawant, T., & Gogle, D.P. Phytochemicals extraction, separation and analysis. Global education limited, 2019.

Pasukamonset, P., Kwon, O., & Adisakwattana, S. (2016). Alginate-based encapsulation of polyphenols from *Clitoria ternatea* petal flower extract enhances stability and biological activity under simulated gastrointestinal conditions. *Food Hydrocolloids*, *61*, 772-779.

Patel, N., Lalwani, D., Gollmer, S., Injeti, E., Sari, Y., & Nesamony, J. (2016). Development and evaluation of a calcium alginate based oral ceftriaxone sodium formulation. *Progress in Biomaterials*, 5, 117-133.

Patil, P., Chavanke, D., & Wagh, M. (2012). A review on ionotropic gelation method: novel approach for controlled gastroretentive gelispheres. *International Journal of Pharmacy and Pharmaceutical Sciences*, 4(4), 27-32.

Pongmalai, P., Devahastin, S., Chiewchan, N., & Soponronnarit, S. (2013). Effect of ultrasonic pretreatment on extractability of glucosinolates from cabbage outer leaves.

Santana, B. R., & Ribeiro, L. F. (2023). Optimization of the extraction of bioactive compounds from *Clitoria ternatea L* and evaluation of encapsulation by ionotropic gelation.

Sharma, M., Dash, K. K., & Badwaik, L. S. (2022). Physicochemical and release behaviour of phytochemical compounds based on black jamun pulp extracts-filled alginate hydrogel beads through vibration dripping extrusion. *International Journal of Biological Macromolecules*, *194*, 715-725.

Stojanovic, R., Belscak-Cvitanovic, A., Manojlovic, V., Komes, D., Nedovic, V., & Bugarski, B. (2012). Encapsulation of thyme (*Thymus serpyllum L.*) aqueous extract in calcium alginate beads. *Journal of the Science of Food and Agriculture*, *92*(3), 685-696.

Tundis, R., Marrelli, M., Conforti, F., Tenuta, M. C., Bonesi, M., Menichini, F., & Loizzo, M. (2015). *Trifolium pratense* and T. repens (Leguminosae): edible flower extracts as functional ingredients. *Foods*, *4*(3), 338-348.

Tzatsi, P., & Goula, A. M. (2021). Encapsulation of extract from unused chokeberries by spray drying, co-crystallization, and ionic gelation. *Waste and Biomass Valorization*, 12, 4567-4585.

Zam, W., Bashour, G., Abdelwahed, W., &Khayata, W. (2014). Alginate-pomegranate peels' polyphenols beads: effects of formulation parameters on loading efficiency. *Brazilian Journal of Pharmaceutical Sciences*, *50*, 741-748.

Zam, W., Bashour, G., Abdelwahed, W., &Khayata, W. (2014). Alginate-pomegranate peels' polyphenols beads: effects of formulation parameters on loading efficiency. *Brazilian Journal of Pharmaceutical Sciences*, 50, 741-748.